J. Plasma Fusion Res. SERIES, Vol. 4 (2001) 387–390

Study of Electrostatic Potential in the GAMMA 10 End Region with Variation of End Plate Resistance

TATEMATSU Yoshinori*, SAITO Teruo, IMAIZUMI Yusuke, NISHIDA Keiichi, YOKOYAMA Eiji, ISHIKAWA Masao, KAJIWARA Ken[1)], KATANUMA Isao and YATSU Kiyoshi

Plasma Research Center, University of Tsukuba

Tsukuba, Ibaraki 305-8577, Japan

[1)]Naka Fusion Research Establishment, Japan Atomic Energy Research Institute

Naka, Ibaraki 311-0193, Japan

(Received: 5 December 2000 / Accepted: 27 August 2001)

Abstract

An experiment of variation of an end plate resistance over several orders of magnitude is carried out in GAMMA 10. The axial potential distribution in the end region is measured for a wide range of an end plate net current. A potential model which calculates a potential distribution in front of a current carrying wall is developed. The potential depth from a mirror throat (B = 3 T) to the end plate (B = 0.01 T) is calculated with this model. The experimental results are well explained by this model.

Keywords:

electrostatic potential, net current, secondary electron, sheath, tandem mirror

1. Introduction

End plates have been installed in front of end walls of the tandem mirror GAMMA 10 and connected to a vacuum vessel with a high resistance R_{EP} of 275 kΩ. They are supposed to control potential formation and suppress non-ambipolar diffusion along magnetic fields. We have developed a potential model for an end region of a tandem mirror on the basis of floating condition of the end plates [1,2]. From comparison of the model calculations with experimental results [3-6], the axial potential distribution in the end region was well reproduced by the model. However, the sheath potential depth in front of the end plate was a little shallower than that expected by the model. A detailed analysis of an experiment, in which secondary electrons emitted from the end plates are suppressed, has been shown that a current balance does not hold and a negative net current enters the end plate even for the standard high resistance case [4].

To investigate the relation between the net current and the potential distribution, we actively broke the floating condition on the end plate by varying the resistance R_{EP} in a wide range [7]. Then we have extended our potential model to include the effect of the net current. This paper describes the extended model and discusses the observed potential distribution in the end region for resistance variation.

In the present paper, the experimental result of end plate resistance variation is described in section 2. The potential model including the effect of the net current is developed in section 3. Then discussion and conclusion follow in sections 4 and 5.

2. Experiment of End Plate Resistance Variation

Fundamental electron cyclotron resonance heating (ECRH) is applied in an end mirror cell for plug

Corresponding author's e-mail: tatema@prc.tsukuba.ac.jp

potential generation. The cell is located inside the mirror throat shown in Fig. 1. The axial profile of the magnetic field strength in the end region is also shown in Fig. 1. The magnetic field strength decreases from 3 T at the mirror throat to 0.01 T on the end plate in the GAMMA 10 end region. Warm electrons created by ECRH and ions flow out of the mirror throat and enter the end plate. They induce a secondary electron emission from the end plate.

A part of warm electron flux out of the mirror throat is reflected by a potential drop in front of the end plate and secondary electrons emitted from the end plate are returned by the magnetic mirror. Ion and warm electron current densities I_i and $-I_e$ are measured with a multi-grid type electrostatic enegry analyzer on the end plate and the secondary electron current density $I_{se} = \gamma I_e$ is evaluated by the secondary electron emission coefficient γ of the stainless steel end wall [4]. The coefficient γ includes the effect of magnetic mirror reflection [4]. The net current density is determined as $I_{net} = I_e - I_i - I_{se}$ on the end plate and $I_{net} > 0$ for electron current excess.

To measure the axial space potential distribution of the end region, Langmuir probes have been installed midway in the end region as shown in Fig. 1. We refer to them as MT-, WI- and WE-probes, respectively. The corresponding potentials are represented as Φ_{MT}, Φ_{WI} and Φ_{WE}. These values are measured in reference to the potential of the vacuum vessel (0 V).

A result of potential measurement for varying end plate resistance is shown in Fig 2. The end plate potential Φ_{EP} is deeply negative for large R_{EP}. It gradually increases as R_{EP} decreases to around 1 kΩ. For small R_{EP}, it approaches to 0 V. Potentials Φ_{MT}, Φ_{WI} and Φ_{WE} behave similarly to Φ_{EP} for the resistance variation. However, they approach positive values for small R_{EP}.

The ratio of the net current to the electron current, I_{net}/I_e, on the end plate is plotted against the end plate resistance R_{EP} in Fig. 3. For large R_{EP}, I_{net}/I_e is small but remains finite, which indicates that the current balance does not hold in front of the end plate. As R_{EP} becomes small, it reaches 0.6.

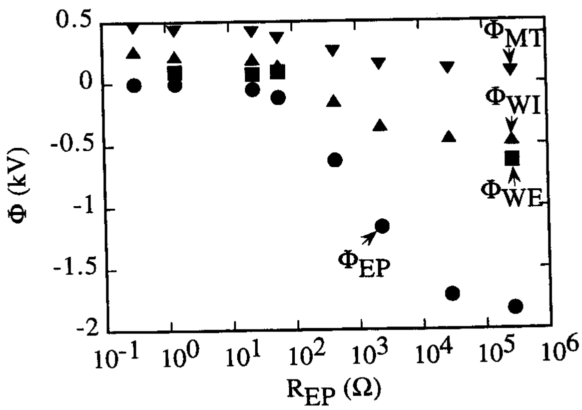

Fig. 2 A result of potential distribution for an experiment of the end plate resistance variation. Potentials are measured in reference to that of the vacuum vessel.

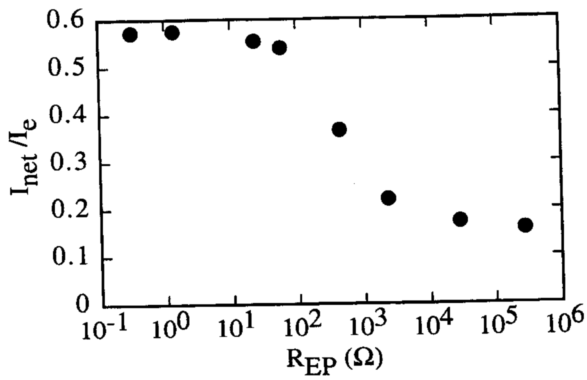

Fig. 3 The ratio of the net current to the warm electron one on the end plate is plotted against the end plate resistance R_{EP}.

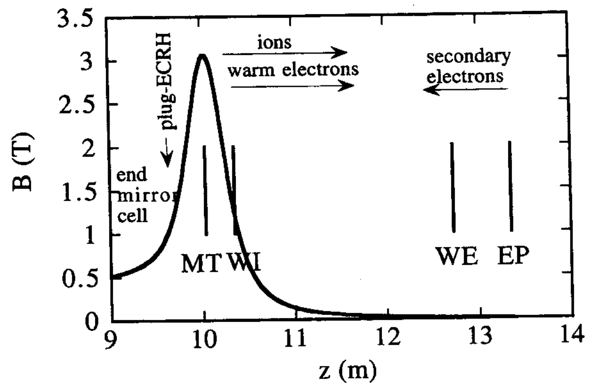

Fig. 1 Distribution of magnetic field strength B in the GAMMA 10 end region. Ions and warm electrons flow out of the mirror throat and secondary electrons are emitted from the end plate (EP). Potential distribution is studied between the mirror throat (MT) and the end plate. To measure axial space potential, Langmuir probes have been installed at the positions marked by MI, WI and WE.

3. Potential Model Including the Net Current

In this section the theoretical potential model [1,2] is extended to include the net current. The model calculates the axial potential distribution between the mirror throat and the end plate.

The potential distribution is determined as follows [2]. Velocity distribution functions of the ions and the warm electrons are given as bi-Maxwellians at the mirror throat and that of the secondary electron is set as a Maxwellian at the end plate. The density and current for each particle species are calculated from the velocity distribution with an assumption of a collisionless plasma. As boundary conditions, current balance on the end plate and charge neutrality, $\rho = qn_i - e(n_e + n_{se}) = 0$, at the mirror throat are imposed, where q and e are the ion and electron electric charges, respectively. An additional condition is the continuity of charge neutrality, $\partial\rho/\partial z = 0$, at the mirror throat. To satisfy all these conditions, ion should have a drift energy corresponding to ion acceleration due to the potential drop from the plug position to the mirror throat. The potential distribution is determined with charge neutrality except a region close to the end plate where a sheath with a width of several times the Debye length is formed.

Here, we permit the net current density I_{net} and introduce a dimensionless parameter,

$$\zeta = \frac{1}{eN_{i0}}\sqrt{\frac{2\pi m}{kT_e}}\, I_{net}\,, \tag{1}$$

where N_{i0}, T_e, and m are the ion density at the mirror throat for the Maxwell distribution, the electron temperature, and the electron mass, respectively. When ζ is positive, the net flow is negative and electron flux exceeds ion flux.

An example of calculated potentials is shown in Fig. 4. as a function of ζ with $\gamma = 0.5$. The normalized potential ψ stands for the potential drop from the mirror throat divided by T_e as $\psi = e(\Phi - \Phi_{MT})/kT_e$. Figure 4 indicates the normalized potentials at the probe positions WI and WE and the end plate EP. As the parameter ζ increases, the normalized end plate potential ψ_{EP} increases, on the other hand ψ_{WE} and ψ_{WI} slightly decrease. The potentials for $\zeta = 0$ agrees with the results calculated with the former model under the floating condition [2].

Variation of the potentials with the net current is explained as follows. When I_{net} is permitted, it does not need to reflect warm electrons in front of the end plate, thus ψ_{EP} increases. For larger ζ, I_i/I_e becomes smaller and ion density becomes smaller than the electron one midway the end region, thus ψ_{WI} and ψ_{WE} go down to keep the charge neutrality by reflecting warm electrons toward the mirror throat and by making the electron density decrease.

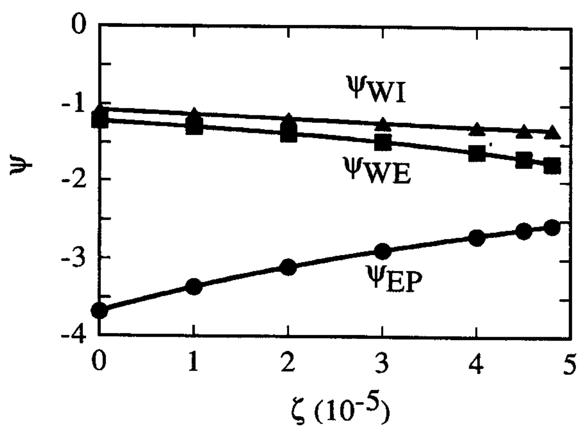

Fig. 4 Calculated normalized potentials with the net current parameter ζ.

4. Discussion

We compare the model calculation and the experimental results by using the following relation between I_{net} and γ,

$$\frac{I_{net}}{I_e} = \frac{\zeta(1-\gamma)}{\zeta + \sqrt{\frac{mT_i}{MT_e}\frac{B_{EP}}{B_{MT}}}}\,, \tag{2}$$

for warm electrons with one component isotropic temperature. Here M is the ion mass, and B_{MT} and B_{EP} is the magnetic field strength at the mirror throat and at the end plate, respectively.

The relation between I_{net}/I_e and $|\psi_{EP}|$ is shown for different values of γ in Fig. 5. The experimental data are also plotted.The model values with $\gamma = 0.5 \sim 0.6$ agree with the data points for $|\psi_{EP}| \simeq 3$ or for a high end plate resistance. This value of γ is consistent with the value evaluated with the stainless steel secondary electron emission coefficient and the magnetic mirror reflection [4,8].

For small $|\psi_{EP}|$, the model value with $\gamma = 0.4$ agrees with the data points. When $|\psi_{EP}|$ is small, potential acceleration of the secondary electrons decreases and the effect of the magnetic mirror reflection increases, thus γ is smaller than that for $|\psi_{EP}| \simeq 3$.

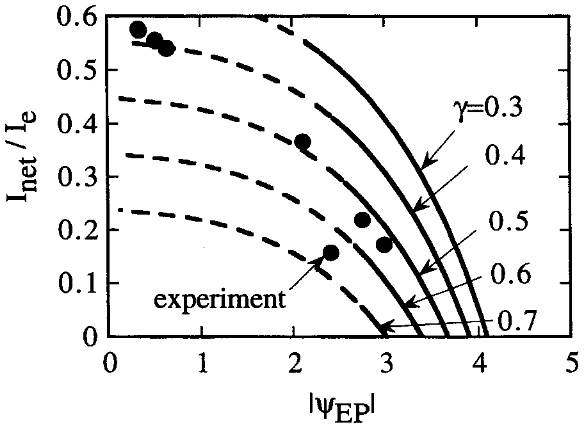

Fig. 5 I_{net}/I_e is plotted as a function of $|\psi_{EP}|$ for different values of γ. The dashed curves indicate the region of non-monotonic solution. The experimental data are also plotted.

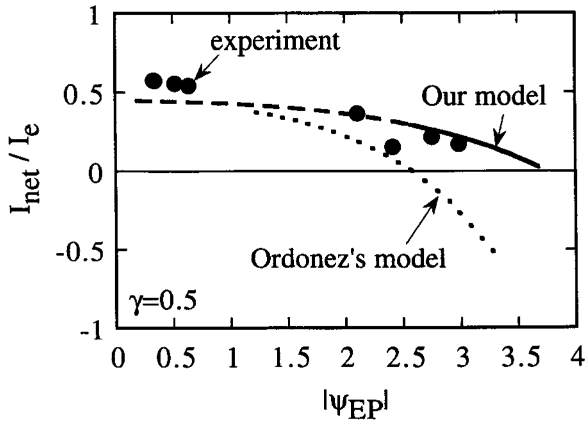

Fig. 6 I_{net}/I_e is plotted as a function of $|\psi_{EP}|$ with $\gamma = 0.5$. Dotted curve is calculated with the Ordonez's model and the solid one is calculated with our potential model. Dashed curve is also the result of our model, however the potential distribution is not monotonic.

The value of I_{net}/I_e is determined by the flux balance, however, the model has no solution of a monotonic potential distribution between the mirror throat and the end plate for small $|\psi_{EP}|$. The dashed curves indicate the region of non-monotonic solution in Fig. 5.

Ordonez has studied a sheath potential including a net current for a non-magnetized plasma [9]. Figure 6 plots I_{net}/I_e calculated with the Ordonez's model against potential depth $|\psi_{EP}|$, which corresponds to ψ_s in Ref [9] for a hydrogen plasma with $T_i/T_e = 0.2$ and $\gamma = 0.5$. The result of our model is also plotted in the same figure. For the Ordonez's model the net current becomes ion excess ($I_{net} < 0$) with $|\psi_{EP}| > 2.6$. In the experiment, the net current is always an electron current for the potential depth of $|\psi_{EP}| \sim 3$. Figure 6 shows that our model is much better fitted to the experimental data than the Ordonez's model though our model has no monotonic solution with small $|\psi_{EP}|$. The reason of this difference is mainly whether the effect of the magnetic field is included or not. More detailed discussion will be carried out elsewhere.

5. Conclusion

A negative net current flows in the end plate in the GAMMA 10 tandem mirror even in the case of a high end plate resistance. The experiment of end plate resistance variation was carried out and the relation between the net current and potential distribution was investigated. The theoretical model including the net current was developed and the experimental results agreed with the model indications. However, small potential depth is attained in the experiment, monotonic solutions with small potential depth are not obtained in the theoretical model.

The authors wish to thank the members of the GAMMA 10 group for stimulating discussions.

References

[1] K. Kurihara *et al.*, J. Phys. Soc. Jpn. **61**, 3153 (1992).
[2] Y. Tatematsu *et al.*, J. Phys. Soc. Jpn. **63**, 558 (1994).
[3] T. Saito *et al.*, Phys. Plasmas **2**, 352 (1995).
[4] K. Kajiwara *et al.*, J. Phys. Soc. Jpn. **66**, 2342 (1997).
[5] Y. Yoshimura *et al.*, J. Phys. Soc. Jpn. **66**, 3461 (1997).
[6] K. Kajiwara *et al.*, J. Phys. Soc. Jpn. **70**, 421 (2001).
[7] T. Saito *et al.*, Tras. Fusion Tech. **39**, 143 (2001).
[8] K. Kajiwara *et al.*, in *Proceedings of 1996 International Conference on Plasma Physics*, edited by H. Sugai and T. Hayashi, Vol.2, 1314 (1997).
[9] C.A. Ordonez, Phys. Fluids B **4**, 778 (1992).